In-situ and triple-collocation based assessments of CYGNSS-R soil moisture compared with satellite and merged estimates quasi-globally

Haotian Wang[a], Qiangqiang Yuan[a,*], Hongfei Zhao[a], Hongzhang Xu[b]

[a]School of Geodesy and Geomatics, Wuhan University, Wuhan, Hubei, 430079, China.

[b]Department of Geography and Environmental Management, University of Waterloo, Waterloo, ON N2L 3G1, Canada.

Email addresses:

haotianw1124@gmail.com (Haotian Wang), yqiang86@gmail.com (Qiangqiang Yuan), zhaohf25@whu.edu.cn (Hongfei Zhao), and h389xu@uwaterloo.ca (Hongzhang Xu).

[*]**Corresponding author:**

Qiangqiang Yuan (yqiang86@gmail.com).

Abstract

Soil moisture is essential for a wide range of agricultural production and climate change. Compared with soil moisture retrieved through satellite remote sensing or merged products, soil moisture products retrieved using the Cyclone Global Navigation Satellite System observations interferometric Reflectometry (CYGNSS-R) have received extensive attention. The soil moisture products retrieved from the CYGNSS-R observation have high temporal and spatial revisit characteristics. In this study, we provide a comprehensive evaluation of CYGNSS-R-based surface soil moisture (SSM), Soil Moisture Active Passive (SMAP) SSM, and the European Space Agency's Climate Change Initiative (ESA CCI) SSM at a quasi-global scale. An in-situ validation based on stations from International Soil Moisture Network and an evaluation strategy based on triple collocation is conducted to comprehensively assess the accuracy of heterologous SSM products. The new evaluation triplet includes the CYGNSS-R-based, merged, and in-situ SSM products TC method (CMID-TC). By analyzing the temporal and spatial distribution of the errors and the distribution in different land cover types, the accuracy of CYGNSS soil moisture product is assessed and compared. Results show that CYGNSS-R-based SSM achieve overall higher absolute accuracy than SMAP satellite-based SSM. CYGNSS-R-based SSM achieved worse accuracy indicators than SMAP SSM in grassland, savanna, shrubland, cropland, and forest land cover and had slightly better accuracy than SMAP in barren pixels. CYGNSS has demonstrated the potential to improve the accuracy of fusion products through its high accuracy and ability to capture temporal correlations in TC analyses. The complementarity in the accuracy and spatial coverage between CYGNSS-R SSM and ESA CCI SSM is shown considering diverse land cover. In general, CYGNSS-R SSM shows the potential to capture higher accuracy and temporal trends in lightly vegetated areas. The TC-based assessments proposed in this study can provide a reference for evaluating the accuracy of soil moisture products and comparing the accuracy of soil moisture from different sources. Furthermore, the error verification results can provide a reference for improving the integration of soil moisture products from different sources by comparing the accuracy in different locations and land cover.

Keywords: Surface soil moisture; CYGNSS; Triple collocation; Evaluation.

1 Introduction

The importance of soil moisture as a part of the global water cycle is indisputable (Entekhabi et al., 1996). Soil moisture is an important component in the earth system that determines the energy exchange process between the land surface and the atmosphere (Legates et al., 2011). It plays an essential role in capturing disaster events, such as drought monitoring (Zhu et al., 2021; Das et al., 2022; Cai et al., 2021), flood warning (Kim et al., 2019; Xu et al., 2021), climate change (Orlowsky et al., 2014), and crop growth (Zhou et al., 2021; Li et al., 2022; Wu et al., 2020). Based on the rapid spatial and temporal change of soil moisture, dynamic monitoring to obtain large-scale soil moisture and an in-depth understanding of the spatiotemporal dynamics of soil moisture is of great significance to help the government formulate plans for rapid response to natural disasters and accurate crop yield estimation (Sishodia et al., 2020; dela Torre et al., 2021; Saeedi et al., 2022).

Since the 1970s, a series of remote sensing satellites or sensors has been launched to detect changes in soil moisture, including passive microwave sensors (e.g., Special Sensor Microwave/Image (SSM/I), Scanning Multichannel Microwave Radiometer (SMMR), Fengyun-3 Weather Satellite, Advanced Microwave Scanning Radiometer–Earth Observing System (AMSR-E), Second Generation Advanced Microwave Scanning Radiometer (AMSR2), Soil Moisture and Ocean Salinity (SMOS), and others) and active microwave sensors (e.g., the Advanced SCATterometer (ASCAT), advanced microwave scatterometer Sentinel-1, and others). Subsequently, Soil Moisture Active Passive (SMAP) emerged as the most recent surface soil moisture (SSM)-dedicated mission, providing active and passive observation products (Entekhabi et al., 2010). Unfortunately, the SMAP radar has failed since

July 7, 2015 (Chan et al., 2016), and only the radiometer remains to operate.

Nowadays, soil moisture products obtained through the inversion of L-band signals from spaceborne Global Navigation Satellite System Reflectometry (GNSS-R) have attracted increasing attention. GNSS-R operates in a bistatic configuration, where the transmitted signal is first scattered forward by the Earth's surface and then captured by a receiver not collocated with the transmitter (Zavorotny et al., 2014). GNSS-R receivers can be low in cost, mass, and power consumption. GNSS-R-based soil moisture products are more affordable, taking advantage of several transmitters that are already in orbit as a part of the GNSS constellation. With a relatively large spatial footprint and frequent observation on the Earth's surface, GNSS-R-based SSM has the potential for contributing higher spatio-temporal resolution to hydrometeorological monitoring, and water resources management. As an early spaceborne GNSS-R observatory, the TechDemoSat-1 (TDS-1) in the United Kingdom provided diverse and large observations supporting retrieval. However, TDS-1 retired at the end of 2019, and it has serious limitations in terms of coverage (Chen et al., 2022). Launched in late 2016, NASA's Cyclone Global Navigation Satellite System (CYGNSS) is able to provide 6-hourly high frequency on a localized Earth-scale revisited observation using eight small satellites orbiting the tropics (Christopher et al., 2019). The CYGNSS has provided a large amount of Earth observation data consisting of frequent geospatial footprints and spatiotemporal revisited observations since 2017 (Christopher et al., 2018; Wang et al., 2018; Gleason et al., 2018). Previous studies focused on obtaining soil moisture products with greater spatial coverage and higher temporal and spatial resolution. Driven by high spatial and temporal resolution data (Xiao et al., 2022; Li et al., 2022; Lee and Kim, 2022; Manoj et al., 2022; Lee et al., 2022), several previous studies on GNSS-R focused on obtaining long-term Cyclone Global Navigation Satellite System observations interferometric Reflectometry (CYGNSS-R-based) soil moisture products (Al-Khaldi et al., 2019; Chew and Small, 2018; Clarizia et al., 2019; Eroglu et al., 2019; Kim and Lakshmi, 2018; Senyurek et al., 2020). CYGNSS Level 3 Soil Moisture Version 1.0 (Chew et al., 2018) is a soil moisture product based on CYGNSS L1 SDR inversion, provided by the University Corporation for Atmospheric Research (UCAR) and the University of Colorado at Boulder (CU). It is the first ubiquitously released CYGNSS-R-based soil moisture product worldwide, which has been distributed by NASA Physical Oceanography Distributed Active Archive Centers (PO. DAAC).

The soil moisture accuracy of CYGNSS-R-based SSM should be comprehensively verified with a wide range of possible methods. Soil moisture accuracy verification is constrained by obtaining reliable estimates of ground-truth soil moisture, making it difficult to obtain large-scale, global-scale true soil moisture measurements (Crow et al., 2012). Although ground-based observation sites provide local, small-scale soil moisture measurements, assessments can be affected by mismatches in spatial scale representation (Draper et al., 2013). Triple collection (TC) (Stoffelen et al., 1998) is a method that can provide error estimates for key environmental variables on the Earth's surface and has been widely used in soil moisture evaluation and assessment (Gruber et al., 2017). The TC method is suitable to be applied to the error assessment of heterologous soil moisture as it forms a set of datasets comprising three collocated and error-independent data for juxtaposition evaluation. Therefore, datasets from three different sources can be cross-referenced. However, the relative error measure is constrained by choice of the true reference dataset and its own multiplicative and additive errors (Crow et al., 2012). Subsequently, extended triple collocation (McColl et al., 2014) can reduce the influence of true observation errors by forming hypothetical true observations without using any of the datasets as the true observation reference.

In our study, the TC method was used to evaluate satellite-based soil moisture from SMAP and soil moisture retrieved by CYGNSS-R and merged soil moisture from European Space Agency’s Climate Change Initiative (ESA CCI). Specifically, a new evaluation triplet is CYGNSS-R-based, merged, and in-situ TC method (CMID-TC). It is provided to incorporate site observations and evaluate CYGNSS-R-based errors on a local scale. We also analyze the error indicators to further evaluate the performance of different products over different land cover types. Based on in-situ and TC evaluations from the perspective of temporal variation and spatial accuracy of soil moisture on a quasi-global (QG) scale, comparing the different performances in various regions and under diverse land cover types may be able to provide new insights for improving GNSS-R-based soil moisture estimates. To our knowledge, this study is the first attempt to use TC to obtain a QG scale CYGNSS-R-based SSM error and correlation evaluation and compare it with SMAP and ESA CCI SSM.

The remaining part of this paper is organized as follows. Section 2 introduces the features of the QG area and the datasets. Section 3 describes the spatial-temporal resampling method, extended triple collocation and non-TC based evaluation metrics for soil moisture assessment. Section 4 presents the assessment results of soil moisture based on CMID-based ETC, discusses the assessment results and error sources of the two strategies, and proposes an outlook for research in the future. Finally, Section 5 concludes the study.

2 Study area and datasets

2.1 Study area

Specifically, the research area is the QG area between 38 °N and 38 °S and between 135 °E and 164 °W because the coverage of CYGNSS soil moisture is the QG area. In this study, the accuracy of CYGNSS-R SSM soil moisture is verified and compared with satellite-based soil moisture and merged soil moisture.

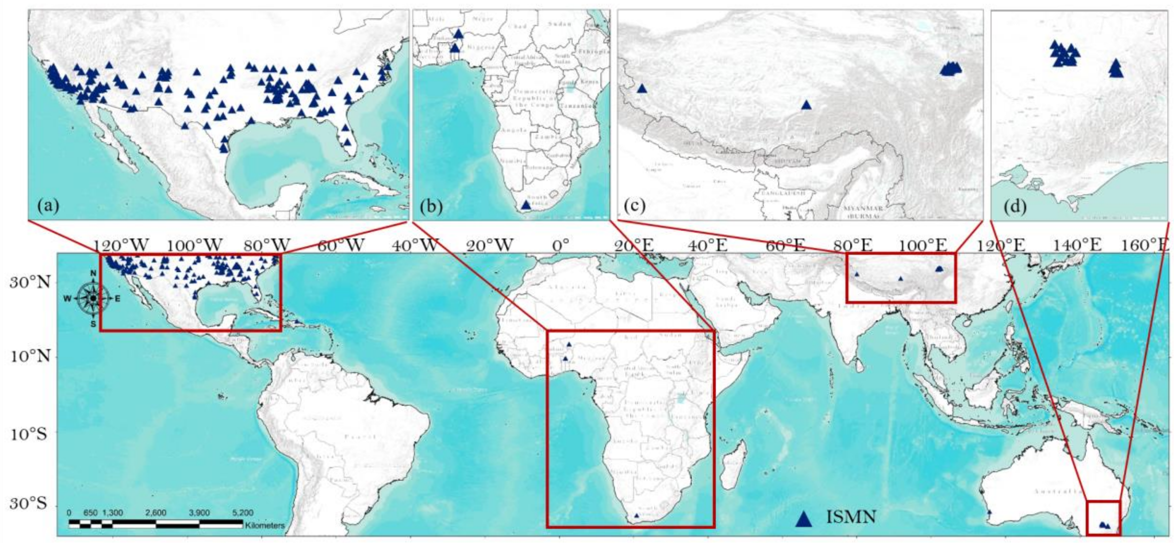

Fig.1. Study area (38 °N ~ 38°S, 135 °E ~ 164 °W) and distribution of the soil moisture in-situ networks. ISMN sites are mainly distributed in (a)North America, (b)Africa, (c)Asia, and (d)Oceania.

2.2 GNSS-R-based SSM retrievals from CYGNSS

CYGNSS Level 3 Soil Moisture Version 1.0 is a GNSS-R-based L-band bistatic radar dataset released by UCAR/CU, providing daily and sub-daily estimates of SSM at a 6-h discretization for most of the subtropics from March 18, 2017, to August 16, 2020 (Chew et al., 2018). This dataset uses a linear regression model between the SMAP soil moisture and CYGNSS reflectivity to solve for daily and sub-daily soil moisture retrieved from effective reflectivity calculated from CYGNSS (Chew et al., 2020). The dataset is gridded to 36-km EASEv2 grids to be consistent with SMAP SSM. The data are archived and can be freely accessed from https://podaac.jpl.nasa.gov.

Owing to the asynchronous nature of the orbits of the GPS transmitters and CYGNSS receivers in the bistatic radar link, temporal sampling is best described by a probability distribution of the revisit time at each location within the ±38° latitude coverage area (Christopher et al., 2019). The median value of the revisit frequency is ~2 h, and the mean revisit frequency is ~6 h.

Traditional remote sensing observations periodically observe a specific location at a specific time in a day in the form of a push-broom cycle, with a consistent revisit frequency. On the contrary, GNSS-R uses ground-reflected signals as observation signals, and the specular reflection points on the Earth's surface are determined by the positions of the transmitting and receiving satellites. The observed footprints formed by GNSS-R on the surface present a statistical pseudo-random distribution and aggregate with the increase of observations to present a complete reflected signal. Therefore, the daily records of GNSS-R SSM represent the soil moisture average for that day.

CYGNSS SSM retrievals are collected from April 1, 2017, to March 31, 2020 for validation. Data records at each 6-hours discretization of time were aggregated to a daily average. Considering that CYGNSS functions as a constellation of passive sensors that receive the signal of surface-reflected GPS pulses (Chew et al., 2020), CYGNSS SSM can be considered as SSM (0–5 cm).

Table 1. Summary of soil moisture used in this study, including in-situ observations, GNSS-R-based, satellite-based and merged SSM.

Source of SSM	Name	# of stations	Available time	Depth(cm)	Temporal resolution
Ground-based in-situ SSM observations	SCAN	239	1996/01/01–2022/02/22	5	Hourly
	SNOTEL	441	1980/10/01–2022/02/22	5	Hourly
	USCRN	115	2000/11/15–2022/02/21	5	Hourly
	AMMA-CATCH	7	2006/01/01–2018/12/31	5	Hourly
	PBO_H2O	159	2004/09/27–2017/12/16	0–5	Daily
	OZNET	38	2001/09/12–2018/08/27	5	Hourly
	MAQU	27	2008/05/13–2019/06/01	5	Hourly
	NAQU	11	2010/06/15–2019/09/12	5	Hourly
GNSS-R-based SSM retrievals	CYGNSS	/	2017/3/17–	Surface	6 h or Daily
Satellite-based SSM retrievals	SMAP	/	2015/3/31	Surface	Daily
Merged SSM	ESA CCI	/	1978/11–2020/12	Surface	Daily

2.3 Ground-based SSM observations from ISMN

The ground-based SSM observations for validation were based on data archived from International Soil Moisture Network (ISMN) (Dorigo et al., 2013). Eight soil moisture observation networks are used in the study, including the Soil Climate Analysis Network (SCAN, Schaefer et al., 2007), the SNOwpack TELemetry (SNOTEL) network (Leavesley et al., 2008), the U.S. Climate Reference Network (USCRN, Bell et al., 2013), the PBO H2O network (Kristine et al., 2008), the OZNET network (Smith et al. 2012), the AMMA-CATCH network (Galle et al., 2018), the MAQU network (Su et al., 2011), and the NAQU network (Su et al., 2011).

The in-situ observations were downloaded from the ISMN website portal:

https://ismn.geo.tuwien.ac.at/en/ from April 1, 2017, to March 31, 2020. A summary of the used in-situ station networks is listed in Table 1 in the supporting information. The ISMN in situ soil moisture measurements from 0-5 cm or 5cm layer were used in the assessment. The quality flag in the ISMN data is applied to select the data points with good quality (Dorigo et al., 2013). The in-situ data are filtered to ensure that at least 100 days of observations are available (Kim et al., 2020).

2.4 Satellite-based SSM retrievals from SMAP

Satellite-based SSM has been available from the SMAP L3 global daily 36-km EASEv2-Grid soil moisture product (SPL3SMP, version 8) since March 31, 2015 (O’Neill et al., 2018). SMAP SSM provide descending-orbit data at 6:00 am and the ascending-orbit data at 18:00 pm. SMAP SSM observations are collected from April 1, 2017, to March 31, 2020, through the NASA National Snow and Ice Data Center Distributed Active Archive Center (NSIDC DAAC): https://nsidc.org/data/SPL3SMP. The SMAP quality flag is used to ensure that only records that are “recommended for retrieval” were used in this study (O’Neill et al., 2015).

2.5 Merged SSM from ESA CCI

Soil Moisture CCI COMBINED Product, Version 05.3(Dorigo et al., 2021) is a merged dataset created as a part of the European Space Agency’s (ESA) Soil Moisture Essential Climate Variable (ECV) Climate Change Initiative (CCI) project. This dataset includes Level 2 scatterometer and radiometer soil moisture products derived from the AMI-WS, ASCAT, SMMR, SSM/I, TMI, AMSR-E, WindSat, AMSR2, SMOS, and SMAP, and fused by defining a uniform standard reference time and temporal resolution. It provides global coverage of SSM at a spatial resolution of 0.25 degrees and at a temporal resolution of daily centered at 0:00 UTC.

In this study, ESA CCI SSM observations are collected from April 1, 2017, to March 31, 2020, through https://www.esa-soilmoisture-cci.org/. ESA CCI SSM are further regridded to 36-km EASEv2 grids to be consistent with CYGNSS-R SSM and SMAP SSM, considering the scale difference between satellite-based, GNSS-R retrieval measurements and merged soil moisture products.

2.6 Auxiliary data

Landcover data were used to analyze soil moisture accuracy under different land cover conditions. MODIS's landcover product MCD12C1 Version 6 (https://ladsweb.modaps.eosdis.nasa.gov/, Friedl et al., 2010) was used to provide landcover information at 0.05-degree spatial resolution at annual intervals. The product provides land cover in six different classification schemes and the IGBP classification scheme is applied in our study. The MCD12C1 product incorporates the 17-class International Geosphere Biosphere Program (IGBP) that is simplified into 6 major types except for Permanent wetlands, Permanent snow and ice, and Water Bodies (Table 4). This study only used the 6 major types for the assessments. In this study, landcover from MCD12C1 are also collected from 2017 to 2020 and regridded to 36-km EASEv2 grids.

Table 2. Detailed information about the landcover used in this study.

IGBP class	Original type	Major type	# of station
1	Evergreen Needleleaf Forest	Forest	17
2	Evergreen Broadleaf Forest		
3	Deciduous Needleleaf Forest		
4	Deciduous Broadleaf Forest		
5	Mixed Forests		
6	Closed shrublands	Shrubland	56
7	Open shrublands		
8	Woody Savannas	Savanna	102
9	Savannas		
10	Grasslands	Grassland	106
11	Permanent wetlands	/	/
12	Croplands	Cropland	32
14	Cropland/Natural Vegetation Mosaic		
13	Urban and built-up land	Barren	19
16	Barren		
15	Permanent snow and ice	/	/
17	Water Bodies		/

3 Methodology

3.1 Spatial-temporal resampling

For each day starting from the time frame center at 0:00 UTC observations within ±12 hours as the time sampling window are considered. First, the daily temporal resolution is chosen as the time baseline, since the temporal resolution of SMAP and ESA CCI SSM products is daily. Although CYGNSS-R-based SSM product provides both 6-hourly and daily temporal resolution products, SMAP and ESA CCI only have soil moisture products with daily minimum temporal resolution. Second, the reference time for the assessment is set at 0:00 UTC to be consistent with the ESA CCI products which are provided at a temporal resolution of daily centered at 0:00 UTC. To be specific, the ISMN in-situ daily soil moisture time series are constructed with respect to the ±12 hours windows centered at 0:00 UTC using all hours of data. The local equatorial overpass time of SMAP SSM is converted to UTC first. Then, the

SMAP daily composite soil moisture estimates are reconstructed within a ±12 hours window centered at 0:00 UTC using their observations from both the ascending and descending modes. CYGNSS-R soil moisture is provided with a 6-hour temporal resolution, starting at 0:00 UTC for every 6-hour period and also reconstructed within a ±12 hours window centered at 0:00 UTC.

These sparsely distributed sites have been widely used to validate grid-based soil moisture (Xu, 2020; Xu et al., 2015; Zhang et al., 2019; Zheng et al., 2022; Xu et al., 2021). To mitigate scaling differences between the point-based in situ measurements and grid-based soil moisture products, in-situ sites that have standard deviations less than 0.1 with CYGNSS soil moisture and ESA CCI soil moisture are removed (Xu et al., 2021). Considering the situation of multiple stations in a sparse grid, the station with the highest correlation with the grid-based soil moisture in the coarse grid is selected (Dorigo et al., 2017).

3.2 Triple collocation

TC method (Stoffelen et al., 1998) is an uncertainty estimation method for estimating the random errors of three mutually independent measurement systems. The premise of the application of this data set is that the data of the three measurement systems are independent and linearly related to the hypothetical true value. Moreover, the errors of the three measurement systems are independent of each other and the hypothetical true value. The linear error model for soil moisture evaluation is presented as follows:

$$\vartheta_i = \vartheta_i' + \varepsilon_i = \alpha_i + \beta_i T + \varepsilon_i \tag{1}$$

where ϑ_i ($i \in 1,2,3$) are three sets of juxtaposed independent measurement systems, corresponding to GNSS-R soil moisture, satellite remote sensing soil moisture products, and in-situ soil moisture or fused soil moisture products. T is the true soil moisture, α_i and β_i are the additive and multiplicative deviations of the dataset relative to the true soil moisture signal in the ordinary least squares modeling, respectively, and ε_i is the additional zero-mean random noise. The error estimation equation for calculating the RMSE of the three groups of soil moisture by TC is obtained by determining the hypothetical true value.

$$\sigma_{\varepsilon_i} = \begin{bmatrix} \sqrt{\sigma_{\vartheta_1}^2 - \frac{\sigma_{\vartheta_1\vartheta_2}\sigma_{\vartheta_1\vartheta_3}}{\sigma_{\vartheta_2\vartheta_3}}} \\ \sqrt{\sigma_{\vartheta_2}^2 - \frac{\sigma_{\vartheta_2\vartheta_1}\sigma_{\vartheta_2\vartheta_3}}{\sigma_{\vartheta_1\vartheta_3}}} \\ \sqrt{\sigma_{\vartheta_3}^2 - \frac{\sigma_{\vartheta_3\vartheta_1}\sigma_{\vartheta_3\vartheta_2}}{\sigma_{\vartheta_1\vartheta_2}}} \end{bmatrix} \tag{2}$$

where σ_{ε_i} is the random error variance of dataset ϑ_i($i \in 1,2,3$). $\sigma_{\vartheta_1}^2$, $\sigma_{\vartheta_2}^2$, and $\sigma_{\vartheta_3}^2$ are the data variance of ϑ_i($i \in 1,2,3$), respectively. $\sigma_{\vartheta_1\vartheta_2}$, $\sigma_{\vartheta_1\vartheta_3}$, and $\sigma_{\vartheta_2\vartheta_3}$ are the covariance of ϑ_1 and ϑ_2; ϑ_1 and ϑ_3; and ϑ_2 and ϑ_3, respectively.

The correlation coefficient can be derived from the measurement system with respect to the unknown target by the extended TC approach (McColl et al., 2014). The unbiased signal-to-noise ratio provides a complementary perspective compared with the RMSE. In addition, extended TC method has the ability to provide different perspectives for verification results.

$$\rho_{T,\vartheta_i}^2 = \frac{\beta_T^2\sigma_{\vartheta_i}^2}{\beta_T^2\sigma_{\vartheta_i}^2 + \sigma_{\varepsilon_i}^2} = \frac{SNR_{ub}}{SNR_{ub} + 1} \tag{3}$$

$$SNR_{ub} = \frac{Var(i)}{Var(\varepsilon_i)} = \frac{\beta_T^2\sigma_{\vartheta_i}^2}{\sigma_{\varepsilon_i}^2} \tag{4}$$

where ρ^2_{T,ϑ_i} is the squared correlation coefficient, and SNR_{ub} is the unbiased signal-to-noise ratio.

3.3 Non-TC based Evaluation metrics

Four metrics are introduced to validate the accuracy of CYGNSS-R-based SSM and other SSM in this study, including Pearson correlation coefficient, root mean square error (RMSE), unbiased RMSE (ubRMSE), and bias. Pearson correlation coefficient is used to measure the degree of linear correlation between site observations and CYNGSS-R-based SSM. RMSE measures the deviation between CYGNSS-R-based SSM and other soil moisture, including in-situ measurements or SSM from different sources. Bias represents the systematic deviation between CYGNSS-R-based SSM and in-situ measurement. UbRMSE is adopted to evaluate the absolute deviation of CYGNSS-R-based and in-situ measurement better as the bias of RMSE is eliminated. These indicators can be calculated as follows:

$$\mathrm{R} = \frac{1}{N-1}\sum_{i=1}^{N}\left(\frac{X_i-\bar{X}}{\sigma_X}\right)\left(\frac{Y_i-\bar{Y}}{\sigma_Y}\right) \tag{5}$$

$$\mathrm{RMSE} = \sqrt{\frac{\sum_{i=1}^{N}(X_i-Y_i)^2}{N}} \tag{6}$$

$$\mathrm{bias} = \frac{1}{N}\sum_{i=1}^{N}(X_i-Y_i) \tag{7}$$

$$\mathrm{ubRMSE} = \sqrt{\frac{\sum_{i=1}^{N}\{(X_i-\bar{X})-(Y_i-\bar{Y})\}^2}{N}} \tag{8}$$

where X_i and Y_i represent two different types of soil moisture data, such as satellite observations and in-situ ground-truth data, N is the total number of observations, $\bar{X}$ and $\bar{Y}$, σ_X and σ_Y represent the mean and standard deviation (SD) of the data, respectively.

4 Results and discussions

4.1 Temporal pattern of soil moisture

Fig. 2 shows the regional average daily SSM over the study period. Generally, the time series fluctuation trends and amplitudes of three soil moisture are relatively similar. The estimated values of CYGNSS SSM and SMAP SSM are closer since a linear relationship between the SMAP soil moisture and CYGNSS reflectivity is used to derive CYGNSS SSM (Chew et al., 2018), which is different from ESA CCI SSM being lower than the other two products in North America, Asia, and South America. In Asia and North America, CYGNSS-R-based SSM can capture evident seasonal changes. In addition, the seasonal variabilities in Africa and Oceania are more volatile, whereas the seasonal variabilities trends captured in Europe are smaller than the ESA CCI SSM, and in South America, seasonal variabilities are gentle.

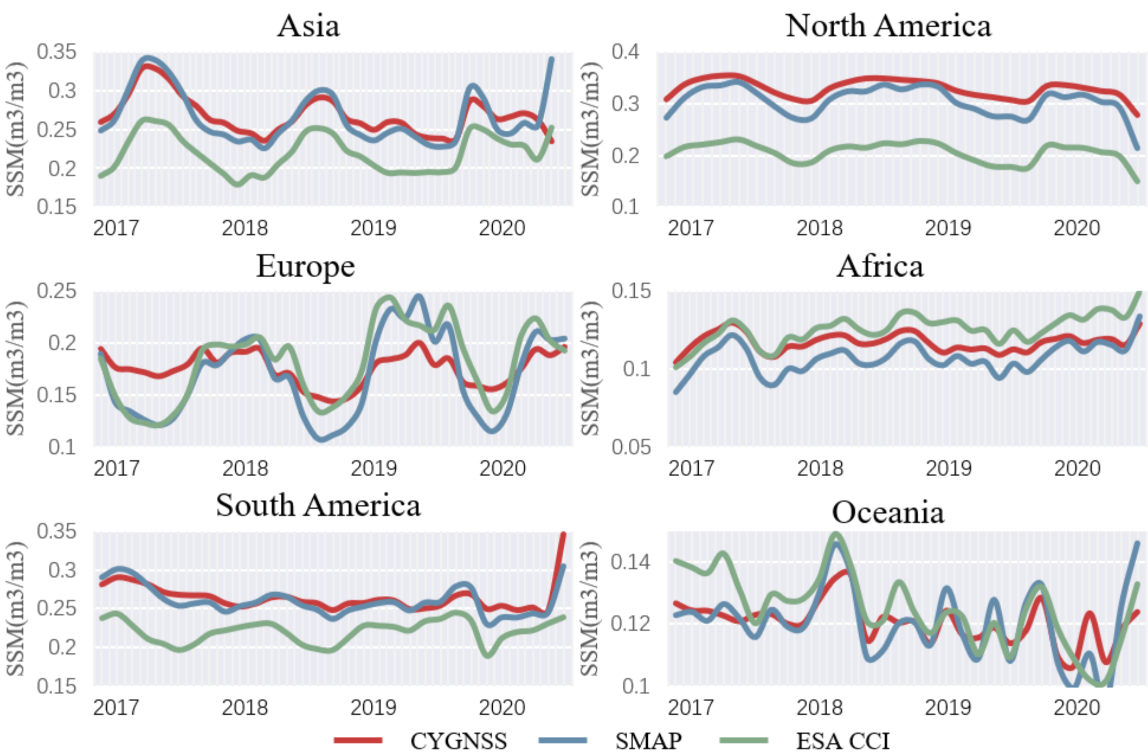

Fig. 2. Regionally averaged daily soil moisture from April 1, 2017, to March 31, 2020.

4.2 In-situ assessment

The results of the validation of the CYGNSS SSM using in-situ sites are given as follows. Fig. 3 shows the box plot of the error validation using site validation for CYGNSS-R-based SSM compared with SMAP SSM with a total of 332 matching valid sites. The cross symbol represents the mean value, and the line in the boxplot represents the median. The correlation of CYGNSS SSM was lower than that of SMAP SSM in all regions. In Asia and Africa, ubRMSE of CYGNSS SSM was higher than that of SMAP SSM. In North America, ubRMSE of CYGNSS SSM was slightly higher than that of SMAP SSM. However, better ubRMSE was achieved in Oceania. RMSE and bias have a similar distribution.

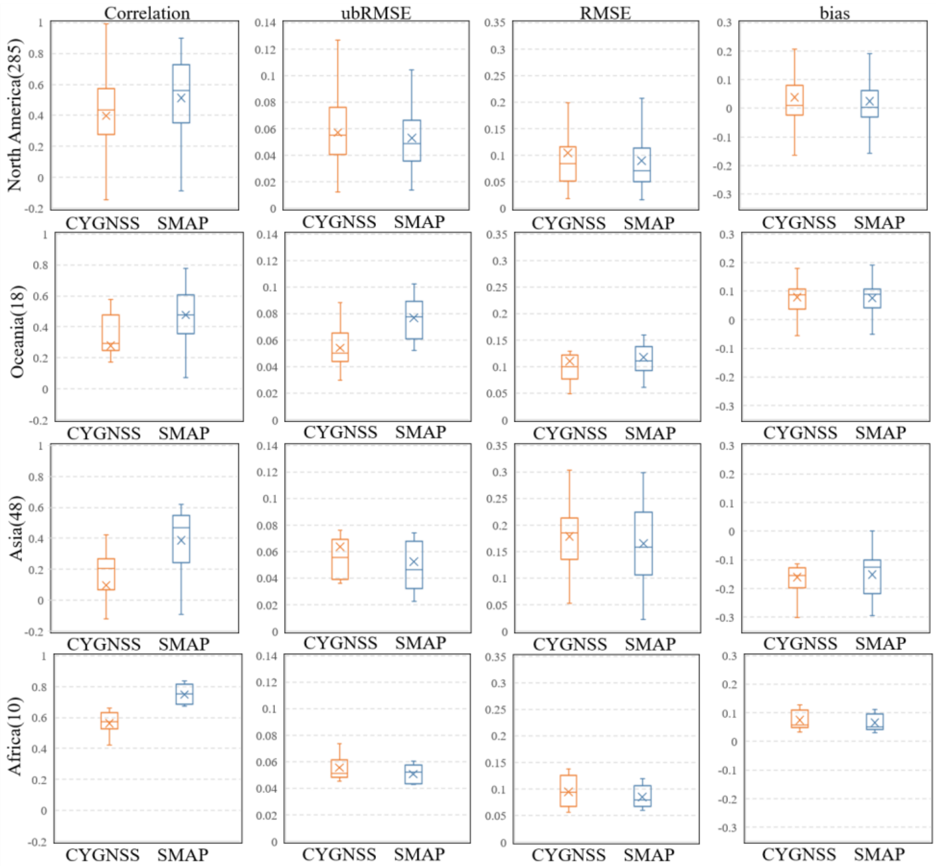

Fig.3. CYGNSS-R-based SSM evaluation based on in-situ stations compared with SMAP SSM from April 1, 2017, to March 31, 2020.

Fig. 4 shows the results of classifying the site verification results of GNSS-R-based SSM according to different land covers. Overall, CYGNSS-R-based SSM has better validation accuracy in cropland and bare land, but there may be overestimation in forested areas. In the GNSS-R soil moisture, open water will have a strong influence on the specular reflection points, so the accuracy of the water mask will affect the inversion results. Optical water masks were used in the CYGNSS-R-based SSM inversion algorithm because the optical data properties underestimate the soil moisture under vegetation.

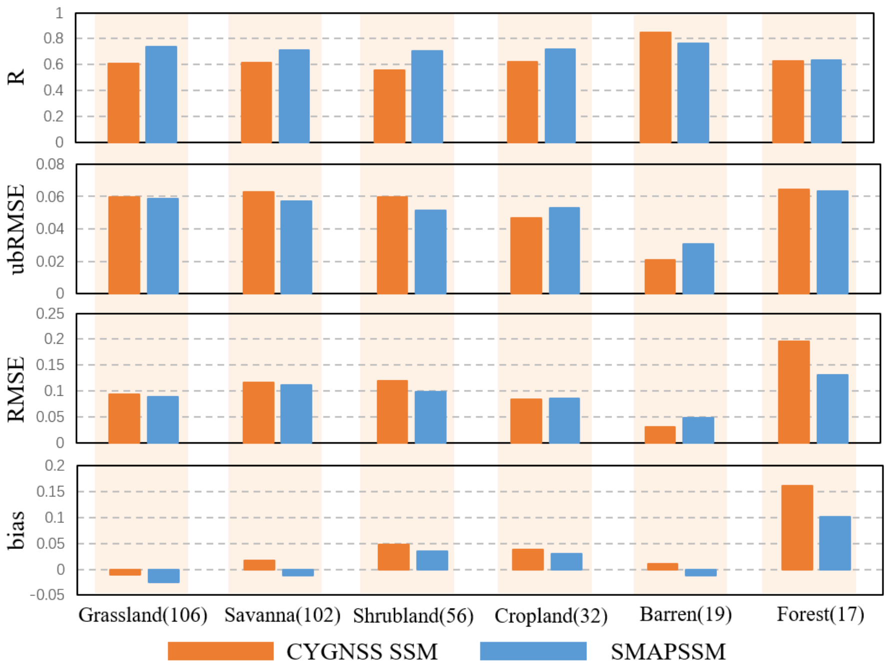

Fig.4. Evaluation metrics on different land covers using in-situ validation for CYGNSS-R SSM and SMAP SSM from April 1, 2017, to March 31, 2020.

4.3 CMID-based TC assessment

The introduction of merged-based SSM into the triplet method can estimate random errors compared with merged soil moisture. Fig.5 shows the error standard deviation (SD) statistic of SSM based on ETC with a combined CMID-based dataset formed from CYGNSS-R-based SSM, merged SSM, and in-situ observations. The SD of CYGNSS-R SSM was higher than that of ESA CCI SSM (with an average of 0.053) in the QG area, with an average SD of 0.069. Low error SD statistic is shown in North America for CYGNSS-R SSM. And a high error SD statistic for CYGNSS-R SSM is seen in Asia, Africa, and Oceania. The influence of ground noise may introduce errors in some specific regions in CYGNSS-R-based SSM. In land calibration, additional empirical calibration of GPS transmit power may cause differences because of error uncertainty (Christopher et al., 2019).

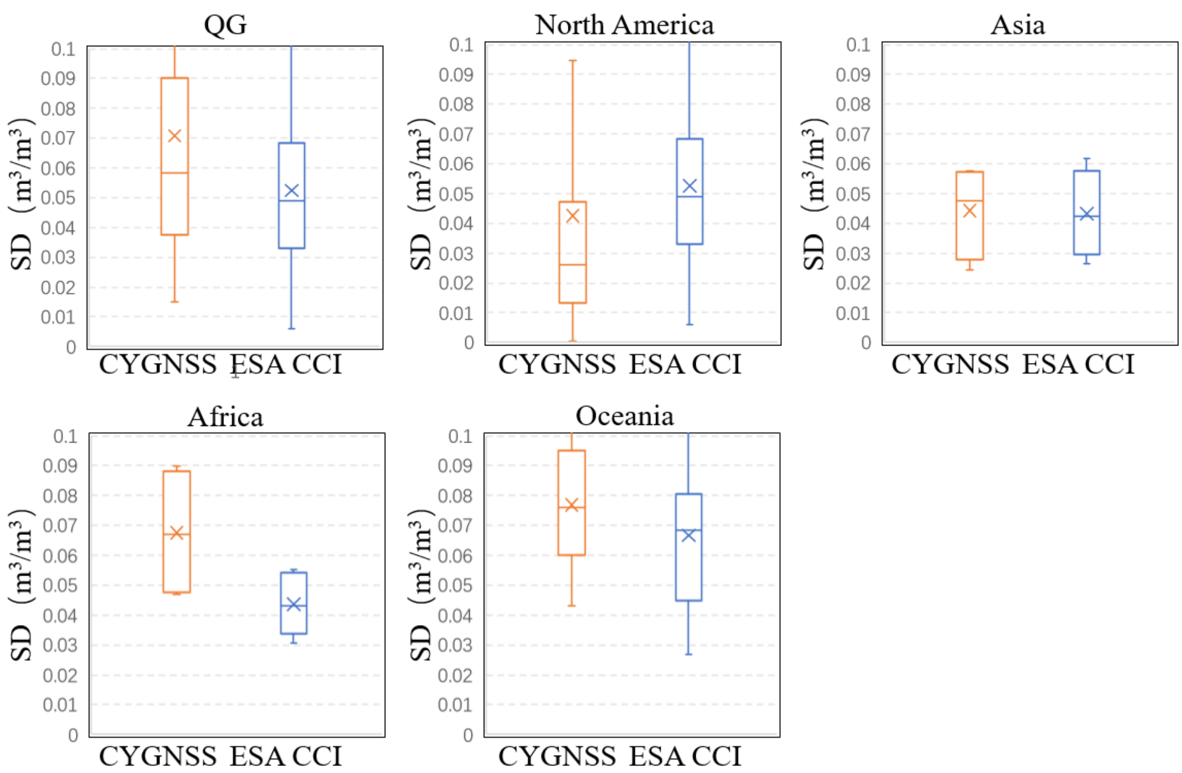

Fig.5. The distribution of SD using CMID-based ETC validation for CYGNSS-R-based SSM and ESA CCI SSM.

Fig.6 depicts the correlation coefficient results obtained by applying the ETC validation on the combined validation dataset for global and regional. CYGNSS-R SSM achieved a relatively higher correlation followed by ESA CCI SSM (0.62), exhibiting an average correlation of 0.64. In North America and Oceania, CYGNSS achieves higher temporal correlations than ESA CCI. The correlation coefficient is generally lower in Asia and Africa than in ESA CCI.

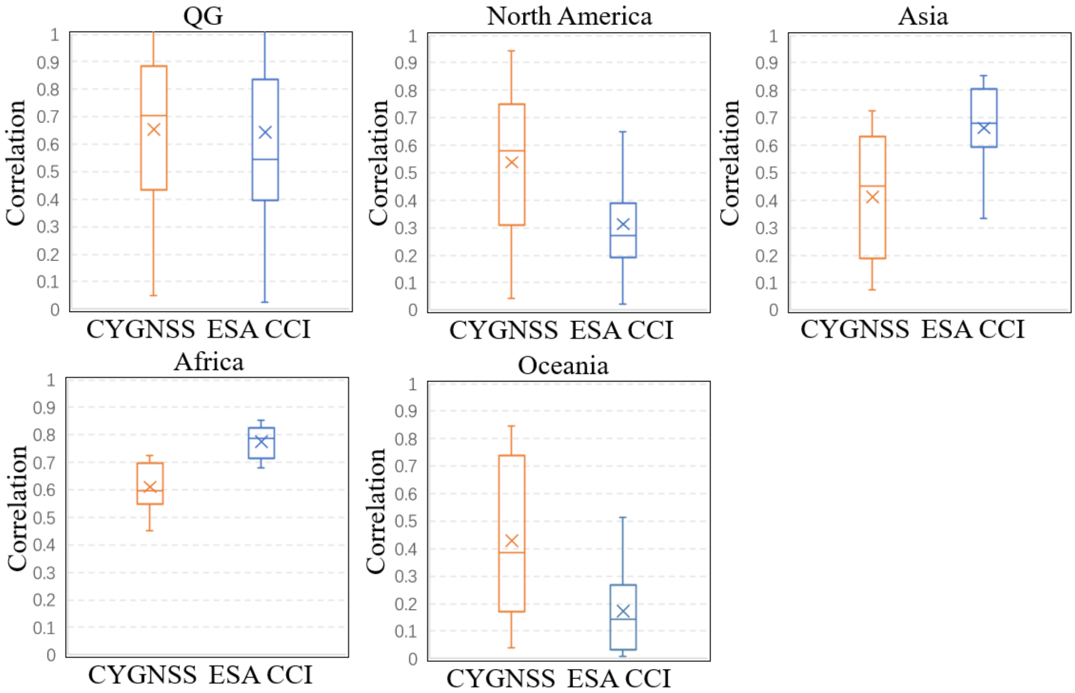

Fig.6. The distribution of correlation coefficient using CMID-based ETC validation for CYGNSS-R-based SSM and ESA CCI SSM.

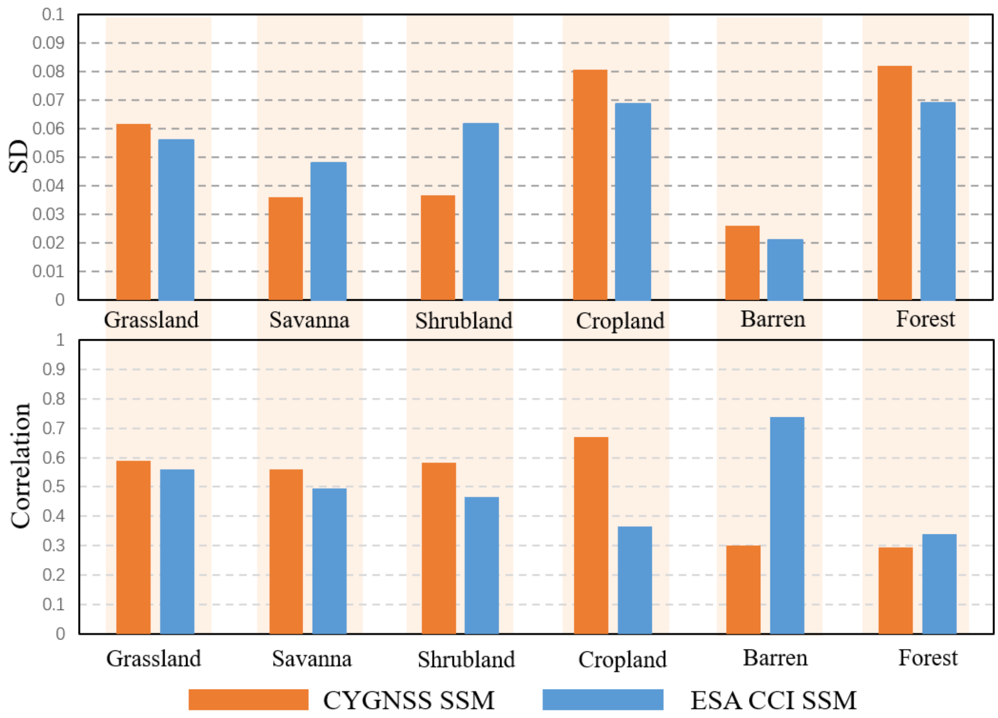

Fig.7. SD and correlation on different land covers using CMID-based TC assessment for CYGNSS-R SSM and ESA CCI SSM from April 1, 2017, to March 31, 2020.

The results of standard deviations and correlation coefficients for different land cover based on the CMID-based ETC are shown in Fig.7. CYGNSS-R SSM demonstrates higher accuracy than ESA CCI over Savanna and shrubland. Low accuracy is seen in the grassland, cropland, forest, and barren. In terms of forests, CYGNSS-R SSM underestimates SSM, which may be greatly affected by the biased surface temperature and other potential factors (Fan et al., 2020). CYGNSS-R SSM obtains a higher correlation coefficient than ESA CCI over grassland, savanna, shrubland, and cropland. In barren and forest, the correlation coefficient was lower than ESA CCI. Overall, CYGNSS-R SSM shows the potential to capture higher precision and temporal trends in lightly vegetated areas.

4.4 Comparison of in-situ assessment and TC analysis

The results of CYGNSS soil moisture based on site verification are similar to the results of the triple combination. The accuracy of CYGNSS SSM is improved but has a relative loss in correlation at the same time. The combination of CYGNSS, ESA CCI, and in-situ supplemented the assessment results of CYGNSS SSM compared with the merged soil moisture source. UbRMSE is adopted to evaluate the absolute deviation as the bias of RMSE is eliminated. The triple collocation analysis can get the random error between the statistical dataset and the ideal reality, and measure the degree of variation or dispersion of the dataset.

The results of the in-situ assessment are also different from those obtained from the CMID-based TC evaluation. The accuracy of CYGNSS is higher than SMAP in in-situ assessment. TC analysis showed that CYGNSS could capture a higher temporal correlation in soil moisture fusion. The correlation coefficients obtained by in-situ assessment and triple combination are different since there are representative errors between point-based observations and grid-based retrievals. Although the sites are sparsely distributed, the triple collocation method deflates the accuracy by inexplicitly utilizing an ideal truth reference. The in-situ assessment results are complementary to the triple combination method in the systematic error estimation at the local scale, as it calculates the absolute error of the dataset.

5 Conclusions

In this study, CYGNSS-R SSM are validated at a quasi-global scale and the accuracy is compared with SMAP and ESA CCI SSM based on in-situ based validation and TC-based evaluation. A triplet dataset composed of CYGNSS-R, merged, and in-situ TC method (CMID-TC) is used to validate and evaluate CYGNSS-R-based SSM based on TC methods. Both in-situ based validation and TC-based evaluation methods are used to analyze the results on different land cover.

Results show that CYGNSS-R-based SSM achieve higher absolute accuracy than SMAP satellite-based SSM. CYGNSS-R-based SSM achieves worse accuracy indicators than SMAP SSM on grassland, savanna, shrubland, cropland, and forest but has slightly better accuracy than SMAP on barren. Hence, less vegetation cover and surface water are allowed for clearer specular points in the surface Fresnel reflection area. The evaluation result of the forest type has relatively bad performance because of the complexity of forest tree morphology and accumulation affecting the GNSS-R signal. Results from TC analysis show that CYGNSS-R SSM outperforms ESA CCI SSM in terms of capturing the temporal trends of soil moisture. The complementarity in the accuracy and spatial coverage between CYGNSS-R SSM and ESA CCI SSM is shown considering diverse land cover. CYGNSS-R SSM obtain higher correlation coefficient than ESA CCI over grassland, savanna, shrubland and cropland. In barren and forest, the correlation coefficient was lower than ESA CCI. In general, CYGNSS-R SSM show the potential to capture higher precision and the temporal trends on lightly vegetated areas. Therefore, CYGNSS has demonstrated the potential to improve the accuracy of fusion products through its high accuracy and ability to capture temporal correlations.

In general, CYGNSS-R-based SSM has great application potential in various land cover because of the high spatial-temporal revisiting observation of CYGNSS. In the future, integration of soil moisture products from different sources can be considered to promote the quality of CYGNSS-R-based SSM and obtain soil moisture estimation with higher accuracy and higher spatio-temporal resolution.

CRediT authorship contribution statement

Haotian Wang: Conceptualization, Methodology, Visualization, and Writing—original draft. Qiangqiang Yuan: Conceptualization, Supervision, and Writing—review and editing. Hongfei Zhao: Conceptualization and Methodology. Hongzhang Xu: Conceptualization and Methodology.

Acknowledgments

This work was supported in part by the National Natural Science Foundation of China (41922008).

References

Al-Khaldi, M.M., Johnson, J.T., O'Brien, A.J., Balenzano, A., Mattia, F., 2019. Time-Series Retrieval of Soil Moisture Using CYGNSS. IEEE Transactions on Geoscience and Remote Sensing 57, 4322–4331. https://doi.org/10.1109/TGRS.2018.2890646

Barrée, M., Mialon, A., Pellarin, T., Parrens, M., Biron, R., Lemaître, F., Gascoin, S., Kerr, Y.H., 2021. Soil moisture and vegetation optical depth retrievals over heterogeneous scenes using LEWIS L-band radiometer. International Journal of Applied Earth Observation and Geoinformation 102, 102424. https://doi.org/10.1016/j.jag.2021.102424

Bell, J.E., Palecki, M.A., Baker, C.B., Collins, W.G., Lawrimore, J.H., Leeper, R.D., Hall, M.E., Kochendorfer, J., Meyers, T.P., Wilson, T., Diamond, H.J., 2013. U.S. Climate Reference Network Soil Moisture and Temperature Observations. Journal of Hydrometeorology 14, 977–988. https://doi.org/10.1175/JHM-D-12-0146.1

Cai, S., Song, X., Hu, R., Leng, P., Li, X., Guo, D., Zhang, Y., Hao, Y., Wang, Y., 2021.

Spatiotemporal characteristics of agricultural droughts based on soil moisture data in Inner Mongolia from 1981 to 2019. Journal of Hydrology 603, 127104. https://doi.org/10.1016/j.jhydrol.2021.127104

Chan S K, Bindlish R, O'Neill P E, et al. 2016. Assessment of the SMAP passive soil moisture product[J]. IEEE Transactions on Geoscience and Remote Sensing, 54(8):4994-5007.

Chen, F., Zhang, X., Guo, F., Zheng, J., Nan, Y., Freeshah, M., 2022. TDS-1 GNSS reflectometry wind geophysical model function response to GPS block types. Geo-spatial Information Science 0, 1–13. https://doi.org/10.1080/10095020.2021.1997076

Chew, C., Small, E., 2020. Description of the UCAR/CU Soil Moisture Product. Remote Sensing 12, 1558. https://doi.org/10.3390/rs12101558

Chew, C.C., Small, E.E., 2018. Soil Moisture Sensing Using Spaceborne GNSS Reflections: Comparison of CYGNSS Reflectivity to SMAP Soil Moisture. Geophysical Research Letters 45, 4049–4057. https://doi.org/10.1029/2018GL077905

Clarizia, M.P., Pierdicca, N., Costantini, F., Floury, N., 2019. Analysis of CYGNSS Data for Soil Moisture Retrieval. IEEE Journal of Selected Topics in Applied Earth Observations and Remote Sensing 12, 2227–2235. https://doi.org/10.1109/JSTARS.2019.2895510

Crow, W.T., Berg, A.A., Cosh, M.H., Loew, A., Mohanty, B.P., Panciera, R., de Rosnay, P., Ryu, D., Walker, J.P., 2012. Upscaling sparse ground-based soil moisture observations for the validation of coarse-resolution satellite soil moisture products. Reviews of Geophysics 50. https://doi.org/10.1029/2011RG000372

Das, P., Zhang, Z., Ren, H., 2022. Evaluating the accuracy of two satellite-based Quantitative Precipitation Estimation products and their application for meteorological drought monitoring over the Lake Victoria Basin, East Africa. Geo-spatial Information Science 0, 1–19. https://doi.org/10.1080/10095020.2022.2054731

Dorigo, W. a., Xaver, A., Vreugdenhil, M., Gruber, A., Hegyiová, A., Sanchis-Dufau, A. d., Zamojski, D., Cordes, C., Wagner, W., Drusch, M., 2013. Global Automated Quality Control of In Situ Soil Moisture Data from the International Soil Moisture Network. Vadose Zone Journal 12, vzj2012.0097. https://doi.org/10.2136/vzj2012.0097

Dorigo, W., Wagner, W., Albergel, C., Albrecht, F., Balsamo, G., Brocca, L., Chung, D., Ertl, M., Forkel, M., Gruber, A., Haas, E., Hamer, P.D., Hirschi, M., Ikonen, J., de Jeu, R., Kidd, R., Lahoz, W., Liu, Y.Y., Miralles, D., Mistelbauer, T., Nicolai-Shaw, N., Parinussa, R., Pratola, C., Reimer, C., van der Schalie, R., Seneviratne, S.I., Smolander, T., Lecomte, P., 2017. ESA CCI Soil Moisture for improved Earth system understanding: State-of-the art and future directions. Remote Sensing of Environment, Earth Observation of Essential Climate Variables 203, 185–215. https://doi.org/10.1016/j.rse.2017.07.001

Draper, C., Reichle, R., de Jeu, R., Naeimi, V., Parinussa, R., Wagner, W., 2013. Estimating root mean square errors in remotely sensed soil moisture over continental scale domains. Remote Sensing of Environment 137, 288–298. https://doi.org/10.1016/j.rse.2013.06.013

Entekhabi, D., Njoku, E.G., O'Neill, P.E., Kellogg, K.H., Crow, W.T., Edelstein, W.N., Entin, J.K., Goodman, S.D., Jackson, T.J., Johnson, J., Kimball, J., Piepmeier, J.R., Koster, R.D., Martin, N., McDonald, K.C., Moghaddam, M., Moran, S., Reichle, R., Shi, J.C., Spencer, M.W., Thurman, S.W., Tsang, L., Van Zyl, J., 2010. The Soil Moisture Active Passive (SMAP) Mission. Proceedings of the IEEE 98, 704–716. https://doi.org/10.1109/JPROC.2010.2043918

Entekhabi, D., Rodriguez-Iturbe, I., Castelli, F., 1996. Mutual interaction of soil moisture state and atmospheric processes. Journal of Hydrology, Soil Moisture Theories and Observations 184, 3–17. https://doi.org/10.1016/0022-1694(95)02965-6

Eroglu, O., Kurum, M., Boyd, D., Gurbuz, A.C., 2019. High Spatio-Temporal Resolution CYGNSS Soil Moisture Estimates Using Artificial Neural Networks. Remote Sensing 11, 2272. https://doi.org/10.3390/rs11192272

Friedl, M.A., Sulla-Menashe, D., Tan, B., Schneider, A., Ramankutty, N., Sibley, A., Huang, X., 2010. MODIS Collection 5 global land cover: algorithm refinements and characterization of new datasets. Remote Sens. Environ. 114 (1), 168–182. https:// doi.org/10.1016/j.rse.2009.08.016.

Galle, S., Grippa, M., Peugeot, C., et al., 2018. AMMA-CATCH, a critical zone observatory in West Africa monitoring a region in transition. Vadose Zone J. 17, 180062. https://doi.org/10.2136/vzj2018.03.0062.

dela Torre, D.M.G., Gao, J., Macinnis-Ng, C., 2021. Remote sensing-based estimation of rice yields using various models: A critical review. Geo-spatial Information Science 24, 580–603. https://doi.org/10.1080/10095020.2021.1936656

Gleason, S., Ruf, C.S., O'Brien, A.J., McKague, D.S., 2019. The CYGNSS Level 1 Calibration Algorithm and Error Analysis Based on On-Orbit Measurements. IEEE Journal of Selected Topics in Applied Earth Observations and Remote Sensing 12, 37–49. https://doi.org/10.1109/JSTARS.2018.2832981

Gruber, A., Dorigo, W.A., Crow, W., Wagner, W., 2017. Triple Collocation-Based Merging of Satellite Soil Moisture Retrievals. IEEE Transactions on Geoscience and Remote Sensing 55, 6780–6792. https://doi.org/10.1109/TGRS.2017.2734070

Gruber, A., Scanlon, T., van der Schalie, R., Wagner, W., Dorigo, W., 2019. Evolution of the ESA CCI Soil Moisture climate data records and their underlying merging methodology. Earth System Science Data 11, 717–739. https://doi.org/10.5194/essd-11-717-2019

Kim, H., Lakshmi, V., 2018. Use of Cyclone Global Navigation Satellite System (CyGNSS) Observations for Estimation of Soil Moisture. Geophysical Research Letters 45, 8272–8282. https://doi.org/10.1029/2018GL078923

Kim, H., Wigneron, J.P., Kumar, S., Dong, J., Wagner, W., Cosh, M.H., Bosch, D.D., Collins, C.H., Starks, P.J., Seyfried, M., Lakshmi, V., 2020. Global scale error assessments of soil moisture estimates from microwave-based active and passive satellites and land surface models over forest and mixed irrigated/dryland agriculture regions. Remote Sens. Environ. 251, 112052 https://doi.org/10.1016/j. rse.2020.112052.

Kim, S., Zhang, R., Pham, H., Sharma, A., 2019. A Review of Satellite-Derived Soil Moisture and Its Usage for Flood Estimation. Remote Sens Earth Syst Sci 2, 225–246. https://doi.org/10.1007/s41976-019-00025-7

Larson, K.M., Small, E.E., Gutmann, E.D., Bilich, A.L., Braun, J.J., Zavorotny, V.U., 2008. Use of GPS receivers as a soil moisture network for water cycle studies. Geophysical Research Letters 35. https://doi.org/10.1029/2008GL036013

Leavesley, G.H., David, O., Garen, D.C., Lea, J., Marron, J.K., Pagano, T.C., Perkins, T.R., Strobel, M.L., 2008. A Modeling Framework for Improved Agricultural Water Supply Forecasting 2008, C21A-0497.

Lee, E., Kim, S., 2022. Spatiotemporal soil moisture response and controlling factors along a hillslope. Journal of Hydrology 605, 127382. https://doi.org/10.1016/j.jhydrol.2021.127382

Lee, J., Park, S., Im, J., Yoo, C., Seo, E., 2022. Improved soil moisture estimation: Synergistic use of satellite observations and land surface models over CONUS based on machine learning. Journal of Hydrology 609, 127749. https://doi.org/10.1016/j.jhydrol.2022.127749

Legates, D.R., Mahmood, R., Levia, D.F., DeLiberty, T.L., Quiring, S.M., Houser, C., Nelson, F.E., 2011. Soil moisture: A central and unifying theme in physical geography. Progress in Physical Geography: Earth and Environment 35, 65–86. https://doi.org/10.1177/0309133310386514

Li, R., Zheng, S., Duan, C., Wang, L., Zhang, C., 2022. Land cover classification from remote sensing images based on multi-scale fully convolutional network. Geo-spatial Information Science 0, 1–17. https://doi.org/10.1080/10095020.2021.2017237

Li, Xuezhang, Xu, X., Li, Xiaohan, Xu, C., Wang, K., 2022. Field scale soil water prediction based on areal soil moisture measurements using cosmic-ray neutron sensing in a karst landscape. Journal of Hydrology 605, 127395. https://doi.org/10.1016/j.jhydrol.2021.127395

Ma, H., Zeng, J., Chen, N., Zhang, X., Cosh, M.H., Wang, W., 2019. Satellite surface soil moisture from SMAP, SMOS, AMSR2 and ESA CCI: A comprehensive assessment using global ground-based observations. Remote Sensing of Environment 231, 111215. https://doi.org/10.1016/j.rse.2019.111215

Manoj J, A., Guntu, R.K., Agarwal, A., 2022. Spatiotemporal dependence of soil moisture and precipitation over India. Journal of Hydrology 610, 127898. https://doi.org/10.1016/j.jhydrol.2022.127898

McColl, K.A., Vogelzang, J., Konings, A.G., Entekhabi, D., Piles, M., Stoffelen, A., 2014. Extended triple collocation: Estimating errors and correlation coefficients with respect to an unknown target. Geophysical Research Letters 41, 6229–6236. https://doi.org/10.1002/2014GL061322

Orlowsky, B., Seneviratne, S., 2014. On the spatial representativeness of temporal dynamics at European weather stations. https://doi.org/10.1002/joc.3903

Ruf, C., Asharaf, S., Balasubramaniam, R., Gleason, S., Lang, T., McKague, D., Twigg, D., Waliser, D., 2019. In-Orbit Performance of the Constellation of CYGNSS Hurricane Satellites. Bulletin of the American Meteorological Society 100, 2009–2023. https://doi.org/10.1175/BAMS-D-18-0337.1

Ruf, C.S., Chew, C., Lang, T., Morris, M.G., Nave, K., Ridley, A., Balasubramaniam, R., 2018. A New Paradigm in Earth Environmental Monitoring with the CYGNSS Small Satellite Constellation. Sci Rep 8, 8782. https://doi.org/10.1038/s41598-018-27127-4

Saeedi, M., Sharafati, A., Brocca, L., Tavakol, A., 2022. Estimating rainfall depth from satellite-based soil moisture data: A new algorithm by integrating SM2RAIN and the analytical net water flux models. Journal of Hydrology 610, 127868. https://doi.org/10.1016/j.jhydrol.2022.127868

Schaefer, G.L., Cosh, M.H., Jackson, T.J., 2007. The USDA Natural Resources Conservation Service Soil Climate Analysis Network (SCAN). Journal of Atmospheric and Oceanic Technology 24, 2073–2077. https://doi.org/10.1175/2007JTECHA930.1

Senyurek, V., Lei, F., Boyd, D., Kurum, M., Gurbuz, A.C., Moorhead, R., 2020. Machine Learning-Based CYGNSS Soil Moisture Estimates over ISMN sites in CONUS. Remote Sensing 12, 1168. https://doi.org/10.3390/rs12071168

Sishodia, R.P., Ray, R.L., Singh, S.K., 2020. Applications of Remote Sensing in Precision Agriculture: A Review. Remote Sensing 12, 3136. https://doi.org/10.3390/rs12193136

Smith, A.B., Walker, J.P., Western, A.W., Young, R.I., Ellett, K.M., Pipunic, R.C., Grayson, R.B., Siriwardena, L., Chiew, F.H.S., Richter, H., 2012. The Murrumbidgee soil moisture monitoring network data set. Water Resources Research 48, W07701. https://doi.org/10.1029/2012WR011976

Stoffelen, A., 1998. Toward the true near-surface wind speed: Error modeling and calibration using triple collocation. Journal of Geophysical Research: Oceans 103, 7755–7766. https://doi.org/10.1029/97JC03180

Su, Z., Wen, J., Dente, L., van der Velde, R., Wang, L., Ma, Y., Yang, K., Hu, Z., 2011. The Tibetan Plateau observatory of plateau scale soil moisture and soil temperature (Tibet-Obs) for quantifying uncertainties in coarse resolution satellite and model products. Hydrology and Earth System Sciences 15, 2303–2316. https://doi.org/10.5194/hess-15-2303-2011

Wang, T., Ruf, C.S., Block, B., McKague, D.S., Gleason, S., 2019a. Design and Performance of a GPS Constellation Power Monitor System for Improved CYGNSS L1B Calibration. IEEE Journal of Selected Topics in Applied Earth Observations and Remote Sensing 12, 26–36. https://doi.org/10.1109/JSTARS.2018.2867773

Wang, T., Ruf, C.S., Block, B., McKague, D.S., Gleason, S., 2019b. Design and Performance of a GPS Constellation Power Monitor System for Improved CYGNSS L1B Calibration. IEEE Journal of Selected Topics in Applied Earth Observations and Remote Sensing 12, 26–36. https://doi.org/10.1109/JSTARS.2018.2867773

Wu, S., Ren, J., Chen, Z., Yang, P., Li, H., 2020. Soil moisture estimation based on the microwave scattering mechanism during different crop phenological periods in a winter wheat-producing region. Journal of Hydrology 590, 125521. https://doi.org/10.1016/j.jhydrol.2020.125521

Xiao, Y., Yuan, Q., He, J., Zhang, Q., Sun, J., Su, X., Wu, J., Zhang, L., 2022. Space-time super-resolution for satellite video: A joint framework based on multi-scale spatial-temporal transformer. International Journal of Applied Earth Observation and Geoinformation 108, 102731. https://doi.org/10.1016/j.jag.2022.102731

Xiao, Y., Su, X., Yuan, Q., Liu, D., Shen, H., Zhang, L., 2022. Satellite Video Super-Resolution via Multiscale Deformable Convolution Alignment and Temporal Grouping Projection. IEEE Transactions on Geoscience and Remote Sensing 60, 1–19. https://doi.org/10.1109/TGRS.2021.3107352

Xu, C., Zhang, S., Zhao, B., Liu, C., Sui, H., Yang, W., Mei, L., 2021. SAR image water extraction using the attention U-net and multi-scale level set method: flood monitoring in South China in 2020 as a test case. Geo-spatial Information Science 0, 1–14. https://doi.org/10.1080/10095020.2021.1978275

Xu, L., Chen, N., Zhang, X., Moradkhani, H., Zhang, C., Hu, C., 2021. In-situ and triple-collocation based evaluations of eight global root zone soil moisture products. Remote Sensing of Environment 254, 112248. https://doi.org/10.1016/j.rse.2020.112248

Xu, X., 2020. Evaluation of SMAP Level 2, 3, and 4 Soil Moisture Datasets over the Great

Lakes Region. Remote Sensing 12, 3785. https://doi.org/10.3390/rs12223785

Xu, X., Tolson, B.A., Li, J., Staebler, R.M., Seglenieks, F., Haghnegahdar, A., Davison, B., 2015. Assimilation of SMOS soil moisture over the Great Lakes basin. Remote Sensing of Environment 169, 163–175. https://doi.org/10.1016/j.rse.2015.08.017

Zavorotny, V.U., Gleason, S., Cardellach, E., Camps, A., 2014. Tutorial on Remote Sensing Using GNSS Bistatic Radar of Opportunity. IEEE Geoscience and Remote Sensing Magazine 2, 8–45. https://doi.org/10.1109/MGRS.2014.2374220

Zhang, R., Kim, S., Sharma, A., 2019. A comprehensive validation of the SMAP Enhanced Level-3 Soil Moisture product using ground measurements over varied climates and landscapes. Remote Sensing of Environment 223, 82–94. https://doi.org/10.1016/j.rse.2019.01.015

Zheng, J., Zhao, T., Lü, H., Shi, J., Cosh, M.H., Ji, D., Jiang, L., Cui, Q., Lu, H., Yang, K., Wigneron, J.-P., Li, X., Zhu, Y., Hu, L., Peng, Z., Zeng, Y., Wang, X., Kang, C.S., 2022. Assessment of 24 soil moisture datasets using a new in situ network in the Shandian River Basin of China. Remote Sensing of Environment 271, 112891. https://doi.org/10.1016/j.rse.2022.112891

Zhou, Q., Ismaeel, A., 2021. Integration of maximum crop response with machine learning regression model to timely estimate crop yield. Geo-spatial Information Science 24, 474–483. https://doi.org/10.1080/10095020.2021.1957723

Zhu, Y., Liu, ·Yi, Wang, W., Singh, V.P., Ren, L., 2021. A global perspective on the probability of propagation of drought: From meteorological to soil moisture. Journal of Hydrology 603, 126907. https://doi.org/10.1016/j.jhydrol.2021.126907